New ways of observing clouds: a tour along satellite based and ground based remote sensing techniques

New ways of

*by André van Lammeren, Dave Donovan, Arnout Feijt,
Robert Koelemeijer and Piet Stammes*

Introduction • On average, more than 60% of the Earth's surface is covered by clouds. Clouds strongly affect atmospheric radiative fluxes and heating rates. Therefore it is crucial that climate models produce realistic cloud fields with the correct cloud properties and feedbacks. This is a challenging task. The underlying difficulty is that many different processes contribute to cloud formation and cloud-radiation interactions at very different scales: e.g. dynamical forcing (large-scale or sub-scale), microphysical processes and cloud geometry with possible overlapping of cloud layers. Although there has been considerable progress in the physical content of the models, clouds remain a dominant source of uncertainty. The Intergovernmental Panel on Climate Change (IPCC) concludes in its latest report [1]: ' ...... *there has been no apparent narrowing of the uncertainty range associated with cloud feedbacks in current climate simulations'*. It is recognised that the only way to make progress in this complex area of atmospheric science is by consistently combining observations with models. This asks for a strong interaction between those making observations and those using climate models [2].

The above implies that cloud observations have to match the modeller's needs. Presently, the available observations are not accurate and detailed enough and do not cover all relevant cloud and aerosol parameters to constrain models adequately.

In this highlight the work within the Atmospheric Research Division on improving cloud observations is presented. This observational programme has been developed in close co-operation with modellers from

KNMI and other institutes. The work includes the development of new ground based remote sensing techniques and the improvement of cloud parameter retrieval algorithms for satellite observations. The measurements are used to derive various cloud parameters such as: cloud base and cloud top height, liquid/ice water path, extinction profiles, total optical depth, albedo and particle size. The retrieved cloud properties are used for a wide spectrum of applications, like model evaluation, monitoring, study of cloud processes, operational use by forecasters, and to improve retrievals of the chemical composition of the atmosphere (e.g. ozone).

In the first part an overview of the retrieval of cloud parameters from operational meteorological satellites is given. Next, a new algorithm for the retrieval of cloud top pressure and effective cloud fraction is presented, based on Oxygen A-band observations of the Global Ozone Monitoring Experiment (GOME). In the last part an innovative synergetic lidar-radar algorithm for the retrieval of particle size and water content for ice clouds is described.

Cloud parameter retrieval with meteorological satellites • Operational meteorological satellites measure reflected sunlight and emitted radiation. These measurements can be used quantitatively to derive cloud properties like: cloud amount, cloud top temperature, optical thickness and water content. In order to derive these cloud characteristics an analysis environment with retrieval algorithms was developed. A large effort was put in the evaluation of the results with synoptic observations and measurements from two measurement campaigns. The satellite platforms used for this study were: the European geostationary satellite Meteosat and the Advanced Very High Resolution Radiometer (AVHRR) on board of the NOAA polar orbiters.

To detect the presence of clouds in the half-hourly METEOSAT images the METEOSAT Cloud Detection and Characterisation KNMI method, MetClock, was developed. The method includes the use of the surface temperature fields of a Numerical Weather Prediction (NWP) model as a dynamic threshold value. Over 2 million synop reports from human observers from all over Europe were used to assess the skill of the method. It was shown that the use of NWP data improves cloud detection significantly.

It was shown that the use of NWP data improves cloud detection significantly

The NWP model surface temperatures are also used in the AVHRR (Advanced Very High Resolution Radiometer) analysis environment called KLAROS (KNMI Local implementation of Apollo Retrievals in an Operational System), developed at KNMI. For the interpretation of the 0.6 mm channel


Discovering clouds

reflectivity, extensive radiative transfer calculations were done with the Doubling-Adding KNMI (DAK) radiative transfer code. The results were put in Look-up tables (LUT). The LUT's are used to obtain the following cloud field properties: cover fraction, optical thickness, emissivity, temperature and liquid water path. In order to assess the quality, the retrieved properties were compared to measurements from two campaigns: the Tropospheric Energy Budget Experiment, TEBEX, and the Clouds and Radiation intensive measurement campaigns, CLARA96, in which the 3GHz radar of Delft Technical University played a central role. The comparison shows that the retrieval algorithms yield results that agree with independent ground based measurements.

The presented case study shows the KLAROS analysis of a frontal zone passage on April 17, 1996. The front passed the Netherlands from the south-west to the north-east. The AVHRR 10.8 mm channel temperatures are displayed in the left panel of Figure 1. The vertical profiles of the 3GHz radar at Delft are shown in Figure 2. The radar measurements support the conceptual model of a warm front. From the overpass of the edge of the front at 8:00 UTC until the time of overpass of the AVHRR (13:00 UTC) the cloud base height decreases from about 7 km to 5.5 km. The clouds at the edge of the cloud field are expected to have a high altitude and a relatively small vertical extent. The AVHRR 10.8 mm channel temperature, however, shows warm clouds at the edge of the frontal zone. This is due to the semi-transparency of thin clouds that causes the signal to be composed of contributions from the cold cloud and the warm surface. KLAROS is employed to correct for the semi-transparency. The retrieved cloud temperatures are presented in the right panel of Figure 1.

From the radar data we estimate the minimum and maximum cloud top height to be 6 and 8 km respectively, which according to radiosonde temperature profiles correlate to cloud top temperatures of 248 K and 233 K. From the cloudy pixels a frequency distribution of measured equivalent black body temperatures at 10.8 mm is made (dashed line in Figure 3). The temperatures range from 240 - 270 K. The average temperature is 259 K, which is well outside of the range of the radar derived temperatures (233 - 248 K). The measured temperatures indicate clouds that occur at altitudes from the ground up to 6.5 km height. Obviously, the 10.8 mm equivalent black body temperatures are not representative for the cloud layer. The solid line in Figure 3 indicates the distribution of corrected cloud temperatures. The values range from 230 to 250 K, which corresponds well with the radar observations. On average the difference between measured and retrieved cloud top temperature is 17 K. In conclusion: KLAROS largely improves the estimate of cloud temperature based on AVHRR data.

The work described above is preparatory to the launch of Meteosat Second Generation (MSG) in January 2002. The passive imager onboard of MSG, the Spinning Enhanced Visible and Infrared Imager, SEVIRI, includes 11 spectral channels, of which 8 are similar to current AVHRR and Meteosat

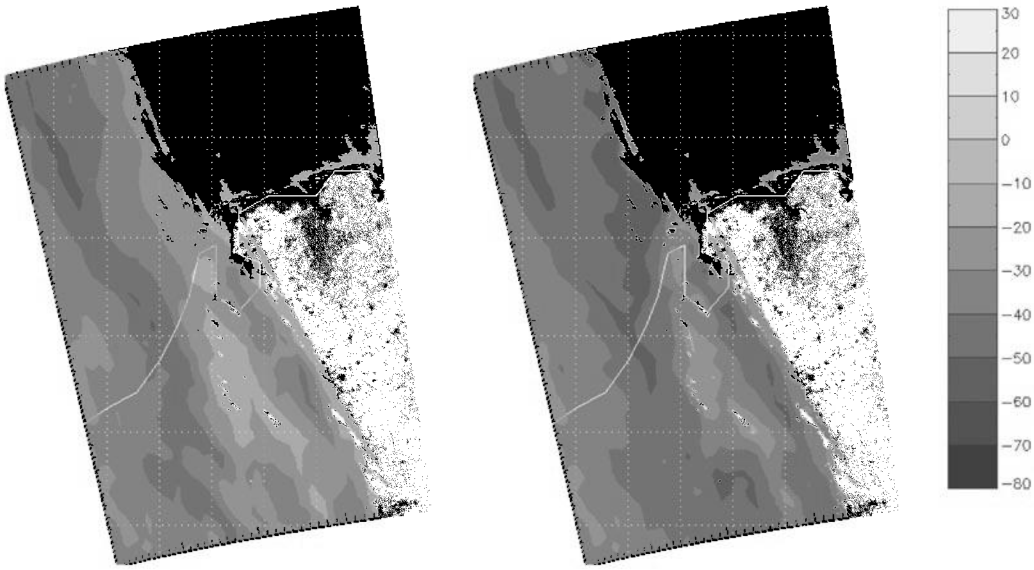

Figure 1 . Measured temperature (left) and retrieved cloud temperature (right) for a frontal zone over the Netherlands. At the eastern edge the temperature difference is 10 to 30 degrees.

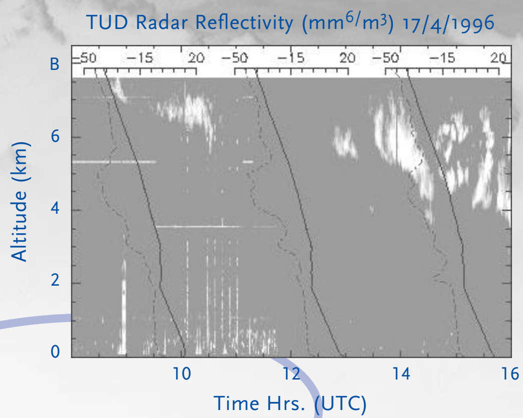

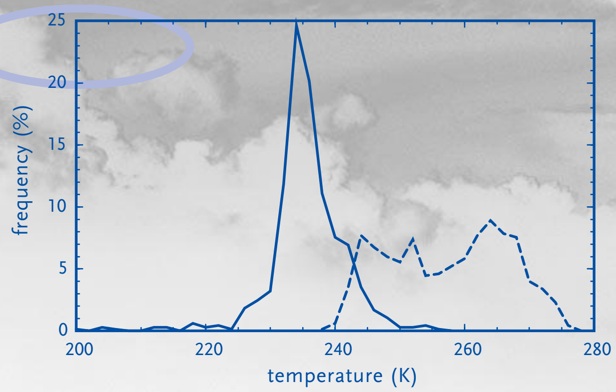

Figure 2. Time series of radar reflectivity. White indicates the presents of cloud particles. The cloud height decreases from 7.5 to about 6 km, which corresponds to temperatures of 233 - 248K.

Figure 3. Frequency distributions of retrieved (solid) and measured (dashed) temperatures near the radar station.

Discovering clouds

channels. SEVIRI enables the retrieval of cloud and surface parameters that are currently derived from Meteosat and AVHRR at a rate of 4 times per hour. This is expected to have a major impact on the meteorological practice and climate research.

Global cloud monitoring with GOME • Global ozone measurements are needed for the study of the chemistry of the atmosphere. To obtain accurate ozone measurements, information on cloud properties is needed because clouds have disturbing effects on the retrieval. Global ozone and cloud observations are obtained from the Global Ozone Monitoring Experiment (GOME) on board ESA's (European Space Agency) ERS-2 (Earth Remote Sensing) satellite. GOME is a spectrometer measuring between 240 - 790 nm. GOME will be succeeded by SCIAMACHY in 2001, and by the GOME-2 instruments in the period after 2005. In the long term, this will yield a measurement record from 1995 till 2015.

Cloud measurement principle • A method has been developed at KNMI to derive effective cloud fractions and cloud top pressures from the spectral reflectivity measurements of GOME. This method, called Fast Retrieval Scheme for Clouds from the Oxygen A-band (FRESCO), makes use of reflectivity measurements in and around the oxygen A-band 3). The oxygen A-band is an absorption band of O_2 near 761 nm, which can be clearly observed in the Earth's spectrum.

The retrieval is based on minimising the difference between a calculated and measured spectrum of the oxygen A-band, by varying the cloud fraction and cloud top pressure in the calculations. In this process cloud optical thickness plays a role. Unfortunately, it is impossible to derive both the cloud fraction and cloud optical thickness independently, because clouds with different optical thickness' and different cloud fractions may give rise to the same spectral reflectivity. Therefore, we assume a cloud albedo of 0.8 (optically thick cloud), and then derive an effective cloud fraction.

The effective cloud fraction is derived from the brightness of the scene with respect to a clear sky scene. The air pressure at the top of the cloud (cloud top pressure) is derived from the depth of the oxygen A-band, which depends on the amount of oxygen above the cloud. For example, if the band is deep, much oxygen is present above the cloud and therefore the cloud top pressure must be high (low altitude cloud). Note that this effective cloud fraction is thus the equivalent cloud fraction holding for an optically thick cloud.

Validation • To validate the effective cloud fractions and cloud top pressures derived using FRESCO, we compared them to cloud properties derived from Along Track Scanning Radiometer (ATSR-2) data that have a smaller pixel size and can well serve as reference. This comparison was made using data acquired over north-west Europe on July 23, 1995. We found that

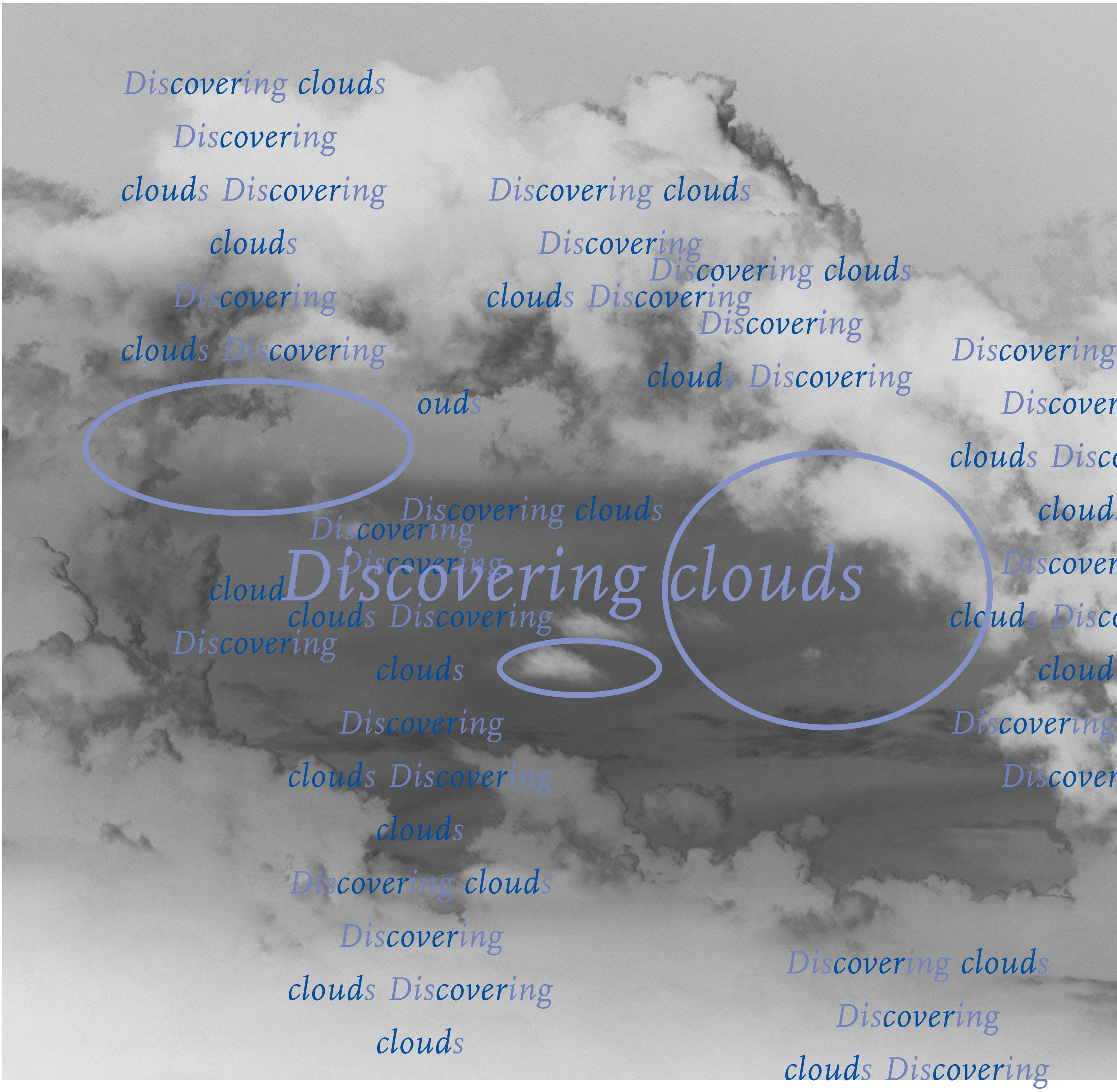
Discovering clouds
Discovering
clouds Discovering
clouds
Discovering
clouds Discovering
Discovering clouds
Discovering
clouds Discovering
Discovering clouds
Discovering
clouds Discovering
Discovering clouds
Discovering
Discovering
Discovering clouds
clouds Discovering
clouds
Discovering
clouds Discovering
clouds
Discovering clouds
Discovering
clouds Discovering
clouds
Discovering clouds
Discovering
clouds Discovering

differences in effective cloud fractions are small, and are mainly introduced by errors in the assumed surface reflectivity. The cloud top pressures derived with FRESCO have an average bias of 65 hPa. This is probably due to absorption by oxygen inside the cloud, which is presently not accounted for in the FRESCO method. Radiative transfer calculations show that this effect can account for this bias [4].

Global monthly average effective cloud fractions and cloud top pressures derived using the FRESCO method for July 1995 are shown in Figures 4a and 4d. For comparison, monthly averaged effective cloud fractions and cloud top pressures from the International Satellite Cloud Climatology Project (ISCCP) are shown in Figures 4b and 4e. The ISCCP data are not yet available for 1995 and onwards, and therefore, a comparison is shown using ISCCP data averaged over the July months of the period 1989-1993. Missing data, e.g. over snow/ice covered surfaces and over high-latitude areas, are shown in black. Figure 4c shows the zonally averaged effective cloud fractions obtained from FRESCO and ISCCP, as well as their difference. Figure 4f shows the zonally averaged cloud top pressures and their difference. The effective cloud fractions of ISCCP are calculated from the cloud fraction and cloud optical thickness, as reported in the ISCCP data set. Clearly, there is agreement between the FRESCO and ISCCP results regarding the main global cloud features, such as low-altitude marine stratus clouds off the west-coasts of large continents, and high altitude convective clouds in the inter-tropical convergence zone (ITCZ). By analysis of time series, seasonal movement of global cloud structures, such as the ITCZ, can be studied.

FRESCO can contribute to the monitoring of cloud top pressures on a global scale

Differences between cloud properties derived using FRESCO and ISCCP are due to various reasons. First, annual (and diurnal) variations explain part of the differences between FRESCO and ISCCP effective cloud fractions and cloud top pressures. Secondly, we want to emphasise that the methods to derive cloud top pressure by FRESCO and ISCCP are very different: FRESCO makes use of near-infrared wavelengths (around 0.76 micron), whereas ISCCP makes use of thermal infrared wavelengths (around 11 micron). Clouds are more opaque at thermal infrared wavelengths than at near-infrared wavelengths. Consequently, the cloud top pressure values derived by FRESCO will be biased towards higher values, because absorption associated with penetration of light into the cloud is not taken into account in the FRESCO retrieval method at present. When further improved, the cloud top pressures derived using FRESCO can be an important contribution to the monitoring of cloud top pressures on a global scale. Knowledge of cloud properties in the atmospheric scene observed by GOME is used to improve column density retrievals of ozone and other trace-gases.

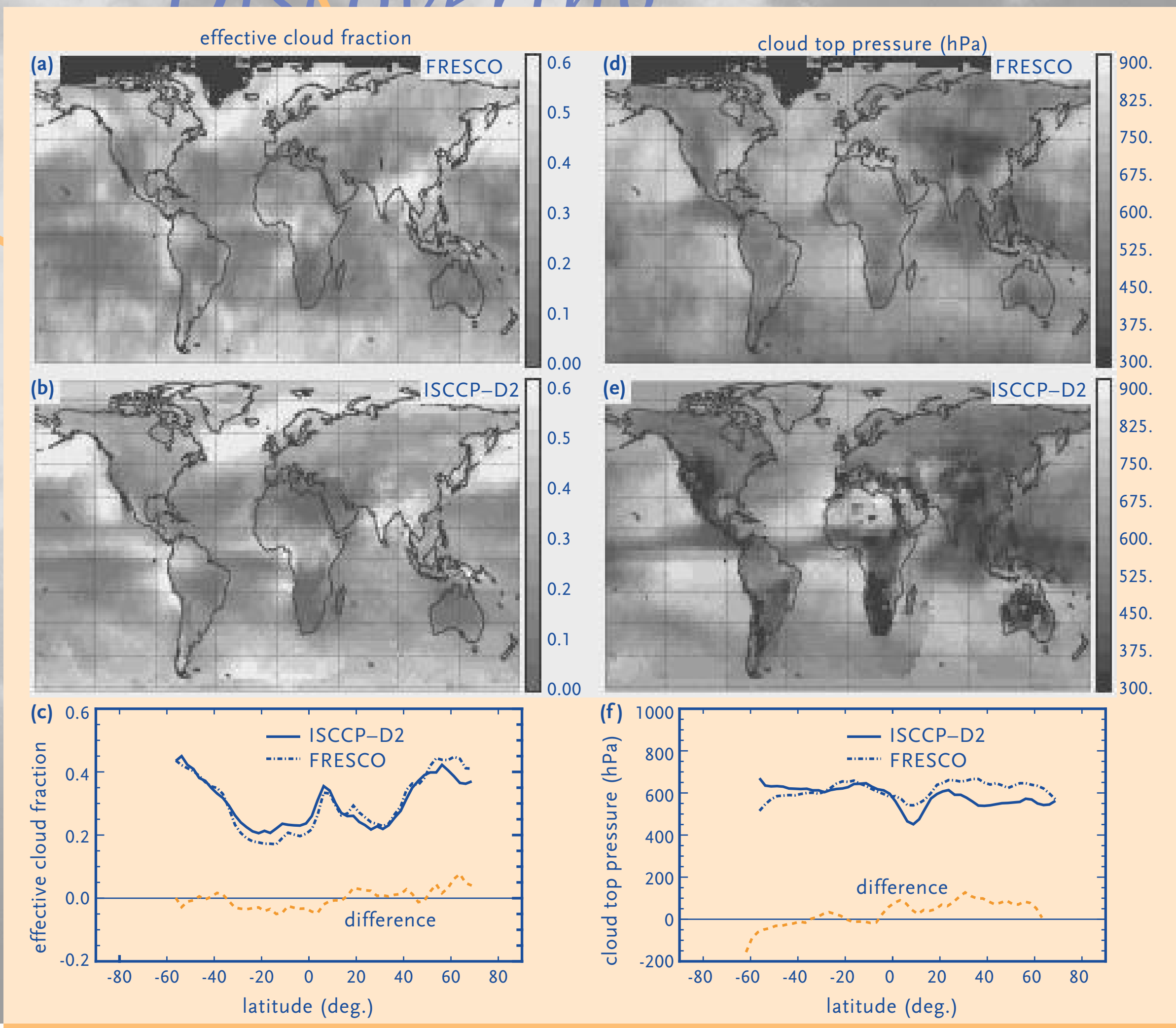

Figure 4. Monthly averaged effective cloud fractions and cloud top pressures derived from GOME using the FRESCO method and from ISCCP. Left: effective cloud fractions, right: cloud top pressures (hPa). Top: FRESCO results, middle: ISCCP results, bottom: zonal averages. The FRESCO results are for July 1995 and the ISCCP results are July-averages of 1989 - 1993.

Combined lidar/radar cloud remote sensing • The present generation of operational meteorological satellites provides insufficient information on the vertical structure of important cloud properties such as cloud cover, optical properties and microphysics. This information can be obtained from ground-based measurements by combining different active and passive remote sensing techniques. In this section we present an example of such a new technique based on the synergy of lidar and radar measurements. It is expected that this newly developed technique will be used for new research satellites in the near future.

Cloud radars and lidar systems operate in a conceptually similar manner. They both transmit a pulse of electro-magnetic radiation into the atmosphere and detect the radiation scattered back to the receiver as a function of time after the pulse has been launched. The key difference between lidars and radars is the very different frequency at which they operate. Lidars usually operate in the wavelength range between 300 and 1000 nm while cloud radars operate in the mm - cm region. This difference in operating wavelength means that a cloud lidar and a cloud radar will be sensitive to different sizes of cloud particles. Roughly speaking, depending on the radar's operating wavelength and sensitivity, cloud radars are mainly sensitive to cloud particles whose characteristic size is greater than 20 - 30 microns, while lidars are mostly sensitive to particles whose characteristic size is below 10 microns. Note in this context that radar reflectivity is proportional to the 6^{th} power of the particle size, and lidar reflectivity only to the second power of the particle size.

Due to the different response to different particle sizes, simultaneous cloud soundings made with a lidar and radar are complementary. For instance, if the particles near the bottom of a cloud happen to be small they may not be detected by the radar, while the lidar will easily detect them. On the other hand, the lidar signal may not reach to the cloud top due to optical attenuation, while the radar signal, being much less attenuated, will reach the cloud top. Putting both the radar and lidar signals together thus often gives a much more complete picture of the structure of clouds.

In parts of the cloud where both the lidar and radar signal is sufficiently strong, the ratio of the optical extinction to radar reflectivity may be determined and used to determine the cloud lidar/radar effective particle radius (R'_{eff}). If assumptions concerning the distributions of particle size and shape are made, the normal effective radius (R_{eff}) used in radiative transfer models of clouds may be determined. At the same time the water content and particle number density may be estimated. These quantities are important in determining the cloud's physical state and how it will interact with solar and thermal radiation within the Earth's atmosphere.

This new procedure to invert combined lidar and radar cloud data has been recently developed at KNMI [5, 6]. Figure 5 shows results obtained during the Clouds and Radiation experiment, which was conducted in the

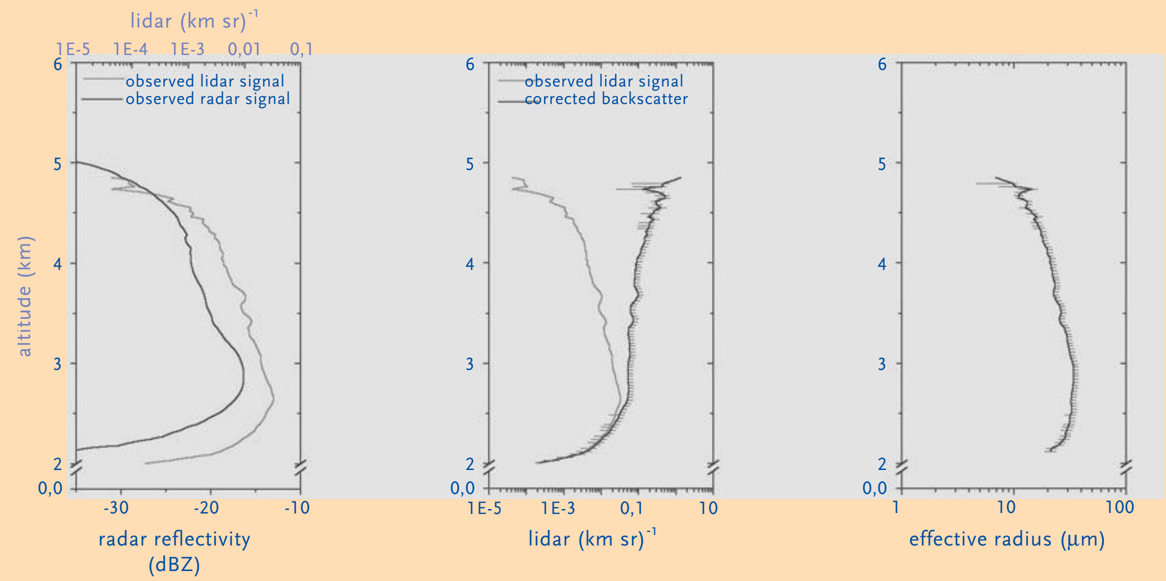

Figure 5. Lidar and Radar signal profiles as well as retrieved optical extinction, water content and effective particle sizes for data obtained during the CLARA campaign.

Discovering clouds

Netherlands in 1996 (CLARA'96). The Figure shows the signal profiles obtained from a mid-level ice cloud together with the retrieved optical extinction, ice-water content and effective radius. The same inversion procedure can be applied to successive signal profiles at fairly high temporal resolution. Figure 6 shows a two-dimensional density plots of the lidar and radar signal fields as well as the retrieved particle sizes and water contents for a 5-hr period on the same day as for the data shown in Figure 5.

The procedure has been applied to a number of situations and a comparison with the results of in-situ aircraft mounted particle probes is very encouraging. Further work is underway to improve the procedure and apply it to large cloud data sets. The results will then be used to develop a better understanding of cloud processes and to improve cloud radiation parameterisation used in atmospheric models. Work is also underway to extent the procedure so that it may be applied to data obtained by space-based lidars and radar missions such as the joint CloudSat (cloud radar) and Picasso (cloud/aerosol lidar) missions of the National and Oceanic Space Administration (NASA) and the proposed EarthCARE (Earth Cloud Aerosol Radiation Explorer) mission of ESA and the National Space Development Agency of Japan (NASDA).

1) Intergovernmental Panel on Climate Change, 2001: *IPCC Third Assessment Report - Climate Change 2001*, UNEP/WMO, in press.
2) Mitchell, J., 2000. *Modelling cloud-climate feedbacks in predictions of human-induced climate change.* In: Workshop on Cloud Processes and Cloud Feedbacks in Large-scale models. World Climate Research Programme, WCRP-110, WMO/TD-No. **993**, Geneva, 2000.
3) Koelemeijer, R. B. A., and P. Stammes, 1999. *Effects of clouds on ozone column retrieval from GOME UV measurements.* J. Geophys. Res., **104**, 8281-8294, 1999.
4) Koelemeijer, R. B. A., P. Stammes, J. W. Hovenier and J. F. de Haan, 2001. *A fast method for retrieval of cloud parameters using oxygen A-band measurements from the Global Ozone Monitoring Experiment.* J. Geophys. Res., to be published.
5) Donovan, D.P. and A.C.A.P. van Lammeren, 2001. *Cloud effective particle size water content profile retrievals using combined lidar and radar observations.* Part I: Theory and simulations. J. Geophys. Res., to be published.
6) Donovan, D.P., A.C.A.P. van Lammeren, R.J. Hogan, H.W.J. Russchenberg, A. Apituley, P. Francis, J. Testud, J. Pelon, M. Quante and J. Goddard, 2001. *Cloud effective particle size water content profile retrievals using combined lidar and radar observations. Part II: Comparison with IR radiometer and in-situ measurements of ice clouds.* J. Geophys. Res., to be published.

Discovering clouds

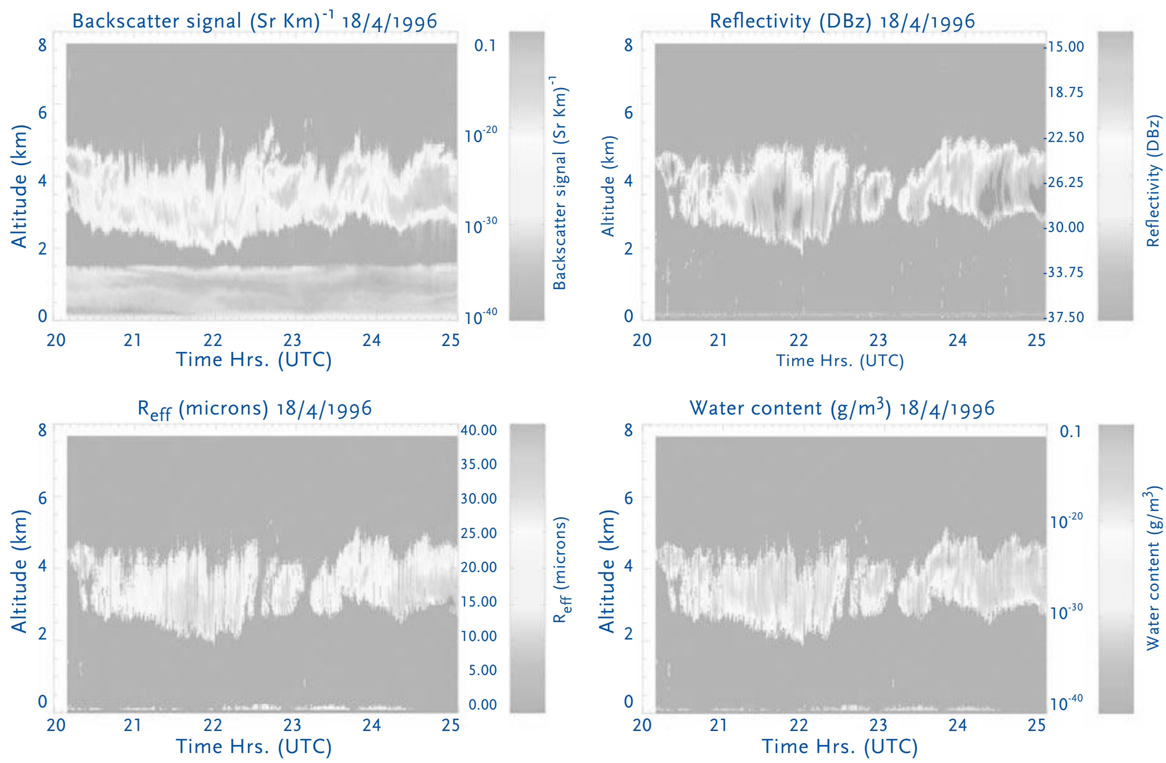

Figure 6. Radar reflectivity (top left), lidar signal (top right), retrieved particle effective radii (bottom left) and Ice water content (bottom right) for April 18th, 1996.